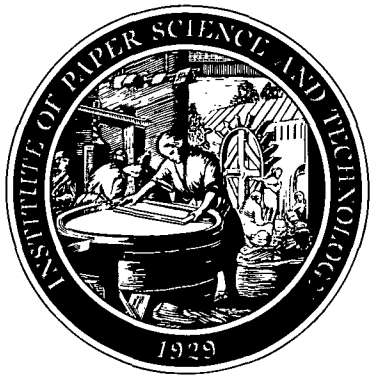

Institute of Paper Science and Technology
Atlanta, Georgia

IPST TECHNICAL PAPER SERIES

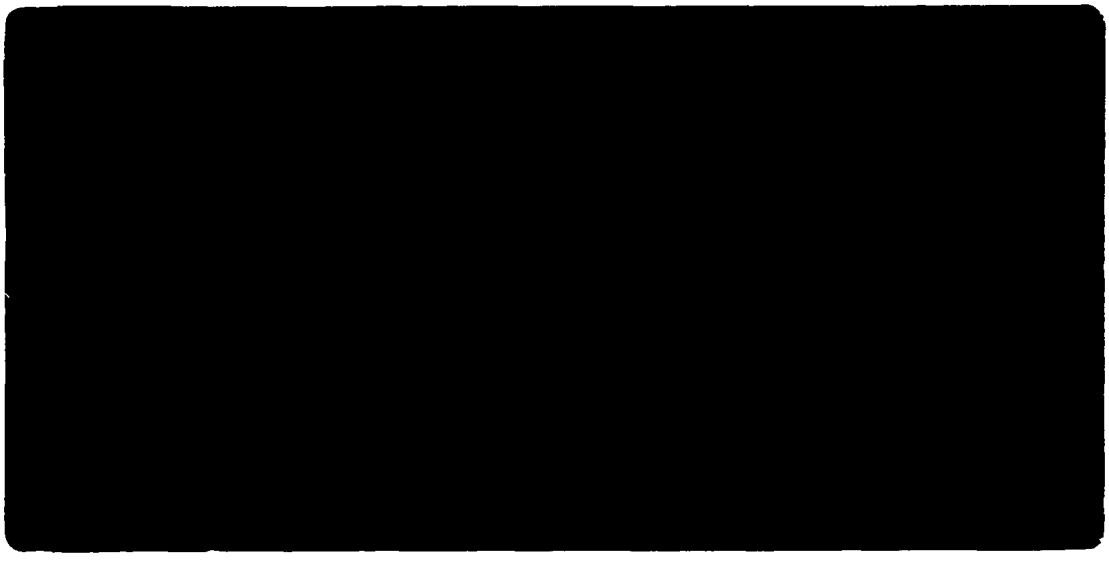

NUMBER 435

THE EFFECTS OF BLACK LIQUOR SPRAY PARAMETERS ON COMBUSTION BEHAVIOR IN RECOVERY FURNACE SIMULATIONS

R.R. HORTON, T.M. GRACE, AND T.N. ADAMS

APRIL 1992

The Effects of Black Liquor Spray Parameters on Combustion Behavior in Recovery Furnace Simulations

R.R. Horton, T.M. Grace, and T.N. Adams

Submitted to
International Recovery Conference
June 7–11, 1992
Seattle, WA

The Effects of Black Liquor Spray Parameters on Combustion Behavior in Recovery Furnace Simulations

Robert R. Horton, Thomas M. Grace, and Terry N. Adams

ABSTRACT

A three-dimensional kraft recovery furnace model has been developed in order to investigate certain critical aspects of the in-flight combustion of black liquor sprays. The model determines the composite behavior of many liquor drops as they move through prescribed gas concentration, temperature, and flow fields in the furnace. Realistic gas flow fields can be developed independently of the combustion simulation. For this study, a flow field was developed which reasonably portrays the flow field observed in isothermal physical models of recovery boilers including features such as recirculation, channeled flow, and flow in a horizontal plane due to jet interaction.

The combustion model describes the in-flight combustion of the black liquor in terms of volumetric rates of drying, volatile release, and char carbon combustion. These rate fields (or clouds) can be characterized in terms of centroids and measures of dispersion. The combustion model also determines the location and state of the black liquor material as it leaves the gas-phase combustion zone, either by landing on the bed, striking a wall, or being carried out the top.

Spray variables which are studied include: mean drop size, breadth of size distribution about the mean, angular width of spray pattern, and angle at which liquor is sprayed into the furnace. The results of these simulations provide quantitative relationships between the spray variables and resultant combustion behavior. Drying zones, volatile release zones, and char burning zones can be defined, and their locations varied as a result of liquor spray parameters.

INTRODUCTION

Combustion of black liquor in recovery furnaces is an extremely complex process. Liquor sprays are characterized by broad spacial distribution and broad droplet size distributions. The resulting individual droplets burn in stages while being acted on by strongly nonuniform gas flow patterns. Direct observation or measurement of this process is frustrated both by the physical size of these process units and by the hostile environment in the lower furnace. Computational techniques to model this type of flow and reaction process have advanced substantially in recent years. However, the geometric intricacies of many small air inlet ports and the complication of multistage in-flight and char bed combustion still limit comprehensive modeling of recovery boilers. In order to circumvent some of this difficulty and gain insight into the interaction between spray combustion and gas flows, an intermediate approach has been developed. This approach makes limited use of Computational Fluid Dynamics (CFD) modeling techniques to develop a furnace gas flow pattern then uses this pattern in a fixed-flow-field to examine the trajectory and combustion of black liquor sprays.

Recovery furnace processes represent very complex applications for CFD techniques. However, without the liquor spray and with nonreacting, isothermal flow, the recovery furnace problem becomes tractable with commercially available CFD codes. The accuracy of the predicted flows can still be tenuous depending on the selection of the grid layout and assumptions concerning turbulence models and other factors. There have been many recent attempts to mathematically model (1-7) and physically model (8-13) recovery furnaces. Many of the larger features of recovery furnace flows are now well established, such as dominantly channeled flow, high velocity horizontal air jets, and multiple recirculation zones. However, neither the detailed flow generated by a specific air system nor an understanding of what constitutes an optimum flow is yet available. For the present purposes, any flow pattern which captures the general recovery furnace features would be suitable for examination of the degree of interaction between flow and black liquor droplet combustion.

Unlike the flow field which must be based on computed results, ample data are now available to accurately model the characteristics of black liquor sprays (14-18). The process of droplet formation from a specific nozzle flow is a complex one which proceeds in stages. The results of this process can be characterized by relative mass distribution with respect to direction from the nozzle centerline and by the size distribution of the resulting droplets. Both of these have been investigated for commercially available black liquor nozzles.

The purpose of this paper is to present the results from the fixed-flow-field model for the impact of spray characteristics on the distribution of black liquor droplet combustion within a recovery furnace. The remainder of the paper is divided into three sections. In the Model Description section, three models will be presented: the isothermal, nonreacting CFD model; the fixed-flow-field combustion model; and the black liquor spray model. Predicted results for a variety of spray conditions will be presented in the Results and Discussion section. Finally, the conclusion derived from the study will be presented in the Conclusions section.

Model Description

Isothermal, Nonreacting, CFD Model

A commercially available CFD code has been used to generate the flow field used in the fixed-flow-field model. The code used was FLUENT v. 3.02 distributed by Fluent, Inc., Lebanon, NH. The description of the geometry and boundary conditions used will be presented below. The case considered involved only the gas flow as there were no sprays or other condensed phase materials specified. The flow was assumed to be nonreacting and isothermal, so calculations involved no heat transfer between the gas and walls or the char bed.

A front and side elevation of the schematic for the CFD model is shown in Figure 1. It shows many of the features found in recovery boilers. The furnace is an open box with a square cross section measuring 10 m x 10 m (32.8 ft. x 32.8 ft.). Only one half of the furnace was modeled due to the assumed symmetry across the vertical center plane running from the front to the back of the furnace. The furnace was modeled only to the level of the bullnose at 30 m (98.4 ft.) which is located on the back wall. The bullnose was taken as a flat horizontal plane blocking 40% of the flow area of the furnace outlet. A solid char bed occupies the floor of the furnace. The char bed surface constitutes lower boundary for computational domain. The edge of the bed at the walls is taken at zero elevation. The bed rises to a maximum elevation of 1.8 m (5.9 ft.) at a distance of 4.2 m (13.8 ft.) from the walls forming a truncated pyramid. Air is injected into the furnace from three elevations. The elevation, number, size, and spacing of the three air levels is given in Table 1.

Table 1. Specification of the Air System Layout.

Air Level	Elevation m (ft)	Number of Ports	Size of Ports cm x cm (in x in)	Spacing
Primary	0.2 (0.66)	Slot	9 cm high (3.9)	Continuous
Secondary	2 (6.6)	6 per wall	33 x 36 (13 x 16.5)	Uniform along wall
Tertiary	8 (26.2)	4 on F/B	33 x 45 (13 x 17.7)	Uniform F/B unl.

The computation of gas flow patterns were carried out using the physical properties for air at 1000°C (1830°F) for the operating conditions listed in Table 2.

Table 20. Specialization of the Air System Operating Conditions.

Air Level	Inlet Velocity mu/s (ft/s)	Approximate injection pressure Pa (inches of H_2O)	Fraction of Total Air
Primary	50 (164)	1000 (4)	35%
Secondary	78 (256)	2000 (8)	45%
Tertiary	83 (272)	3000 (12)	20%

The computational domain was defined as a 32 x 17 x 62 grid (33,728 nodes) using a nonuniform grid. The k-ϵ turbulence model was used, and the solution converged in approximately 10 hours so that the sum of the residuals was less than 10^{-3}. The computer used was an IBM RISC Workstation model 6540 using the AIX operating system.

Output from a CFD calculation involves a very large amount of information: the three components of gas velocity, the pressure, the turbulent energy and dissipation rate of turbulence each for all nodes in the computational field. For the present purposes of obtaining a fixed-flow-field, only the three components of velocity were used. Resulting flow patterns showed some of the features observed in physical models of recovery furnaces: channeled flow and recirculation zones near the walls. Figure 2 shows the constant velocity magnitude contours for a vertical plane running front-to-back and slicing through the line of tertiary air ports closest to the center plane of the furnace. The tertiary jets are quite visible, and the recirculation zone particularly on the back wall is visible.

The velocity contours give a somewhat misleading impression of the smoothness of the flow. For comparison, several parcels of secondary air have been traced in Figure 3. These traces show the path taken by the 10 small parcels of secondary air as they enter the furnace and are affected by the overall flow and turbulence. Their flow paths are varied and complex. Some go smoothly up and out, but most are strongly affected by turbulent motion and by the tertiary air flow.

Gas flow in the center of the furnace had velocities with large upward velocity components. This feature has been referred to as a high velocity central core or as a chimney effect. In order to further characterize the central core, Figure 4 shows the upward component of velocity plotted versus the horizontal position for three locations in the furnace: one just below the liquor guns at 5 m elevation, above the tertiary air ports at 15 m, and another at 25 m just before the bullnose. Upward velocity components as high as 30 m/s were observed in the CFD flow field simulations in the center of the furnace geometry.

Fixed-Flow-Field Combustion Model

The fixed-flow-field was taken directly from the CFD results. Only the three velocity components were used. As a result, the motion of the droplets from the black liquor spray is unaffected by random turbulence. This results in smoother path lines for the droplet trajectories, but there is a potential that the drag and combustion rate could be affected by this. Future work will examine the influence of turbulence on the droplet trajectories predicted by the fixed-flow-field model.

For the results reported here the gas temperature was taken as 1000°C (1830°F). All gas properties used in the calculation of droplet drag are based on the properties of air at this temperature. All three stages of black liquor droplet combustion are dependent on the surrounding gas temperature. Because of this, the assumption of uniform gas temperature at 1000°C (1830°F) somewhat limits the direct applicability of the results. However, this temperature is near that prevailing in recovery furnaces so that trends and sensitivities to spray parameters should be reasonably portrayed.

The black liquor droplet combustion model used here closely follows that proposed by Frederick (19). Some modifications were made in order to account for radiation exchange between the droplet and the surrounding gas and to account for the potential interference between the char oxidation reaction and the char gasification reactions. These modifications are fully discussed elsewhere (20).

Several parameters in the equations for black liquor droplet combustion are user specified. The values used here are listed in Table 3. These were derived from extensive comparison to data on individual black liquor droplet combustion.

Table 3. Model Parameters Used in Fixed-Field Combustion Simulations.

Firing Solids	= 65%
Volatiles Mass Fraction	= 45% (based on total solids)
Char Mass Fraction	= 10% (based on total solids)
Inorganic Mass Fraction	= 45% (based on total solids)
Firing Temperature	= 100°C
Solids at Ignition	= 95%
Gas Temperature	= 1000°C
Gas Emissivity	= 0.4
f, fraction of CO as comb. prod.,	= 0 (All O_2 forms CO_2)
α, O_2 that reads w/ CO H_2	= 1 (only excess O_2 penetrates)
Gas phase composition	
O_2	= 5%
H_2O	= 20%
CO_2	= 12%
N_2	= 63%
Fixed Velocity Field	= Mark 1

Black Liquor Spray Model

In this work, black liquor spray patterns are described by a droplet diameter distribution function, nozzle exit velocity, vertical angle, and a mass flow distribution according to angle. This spray model is based on research data reported in recent IPST black liquor spray studies. The particular model used here describes a typical splashplate black liquor nozzle where the horizontal spread of the spray (spray width) is large, but only a single vertical firing angle is specified. This is depicted in Figure 5.

It has been found that black liquor sprays from commercial nozzles follow a square-root normal size distribution. These are usually characterized in terms of a mass-median-diameter, D_M, and a standard deviation, σ. The breadth of the distribution could be more readily understood in terms of the maximum and minimum diameter. The nature of normal distributions makes it difficult to identify the actual maximum and minimum, so the diameters corresponding to 1.0% and 99% of the mass will be used instead. These will be designated as D1 and D99. A typical value of the median diameter, D_M, is 2.5 mm. For typical black liquor sprays, the values of D1 and D99 would be 0.72 mm and 5.34 mm, respectively.

In order to study the effects of the breadth of the droplet size distribution, the standard deviation was increased or decreased by multiplying by a factor, sf. Values of $sf > 1$ lead to broader distributions, while $sf < 1$ leads to narrower distributions.

Diameters of discrete sizes were specified so that they represented an equal mass fraction of the spray. In the simulations reported here, 20 different droplet diameters were specified, each containing 5% of the total mass of the black liquor spray.

Black liquor sprays have been found to have mass flow rates that are a function of horizontal spray angle, Φ. In this work, a parabolic mass flow profile which gives the fraction of the mass flow as a function of the lateral angle, Φ, was used according to the relationship:

$$\text{mass flow} = 1.537 - 0.000221 \times \Phi^2$$

RESULTS AND DISCUSSION

Simulation Parameters Investigated

This work investigates the effects of several black liquor spray parameters on black liquor combustion. These parameters are mass mean diameter, width of horizontal spray, vertical angle of spray injection, and individual droplet diameters.

The individual effects of changes in each of these parameters about an arbitrary base case is examined as a preliminary study of sensitivity. It is recognized that these parameters will have coupled or interacting effects on combustion behavior; however, the compound effects of varying two parameters simultaneously are not examined here. A more complete study in the future will examine the interaction of these variables and the potential for optimizing firing parameters.

Base Case Description

The base case simulation was chosen to represent typical operating conditions in a recovery furnace. A relatively wide spray pattern was specified, $\Phi = 70°$ (total 140° spray angle) with 57 discrete angles (2.5° separation). A mean diameter of 2.5 mm was used with a distribution of 20 individual droplet sizes. A total of 1140 droplets (57 discrete angles x 20 discrete diameters) were used to represent a spray from each of four nozzles, one in the middle of each wall at 6 m elevation. Base case conditions are summarized in Table 4.

Table 4. Base Case Black Liquor Spray Parameters.

Liquor velocity	10 m/s
Vertical angle	-10°
Horizontal spray width	-70° to +70°, 57 discrete angles
Droplet size distribution	square-root normal
Median droplet diameter, D_M	2.5 mm
Diameter with 1.0% mass less than, D1	0.72 mm
Diameter with 99% mass less than, D99	5.34 mm
Nozzle location	1 per wall, center, 6 m elevation

Simulation Output

The recovery furnace fixed-field simulations calculate the combustion product released into each cell of the grid. For the combustion simulations presented here, a uniform 30 x 30 x 60 grid was used on a 10 x 10 x 30 m furnace geometry so that each cell had dimensions of 0.33 x 0.33 x 0.5 m. Four output arrays contain the sum of mass released from all individual droplets for each stage of combustion for each cell. Additional boundary arrays sum the droplet mass that strikes the walls for each of the four combustion stages. The model does not consider in-flight reactions of smelt, so all inorganic mass in the original black liquor ends up on one of the boundaries: the char bed, one of four walls, the bull nose, or the outlet. At the end of each simulation, the sum of component mass released into each cell is normalized with respect to the total component mass of the entire black liquor spray. This means that each of the four arrays including boundaries will sum to 1.0. The in-flight results can be thought of as normalized rates of evaporation, devolatilization (pyrolysis), or char burning at each location having units of lb./cell/hr per lb. total B.L/hr.

The in-flight combustion rate arrays can be plotted using visualization software which displays three dimensional perspective views of the data which resemble color-coded clouds. Each point of the cloud would have an intensity and location corresponding to the magnitude of mass transferred and the cell location with a different color corresponding to each of the four stages of black liquor combustion. Figure 6 shows results for the base case for water, pyrolysis, and char combustion.

The three-dimensional data are often easier to interpret if presented in two dimensional format. This can be done by summing the data at each horizontal plane and graphing this as a function of vertical position in the furnace. The base case combustion results are presented in this manner in Figure 7. It is observed in this graph that most evaporation takes place in a narrow vertical distance between 5 and 6 meters, while pyrolysis (devolatilization) and char burning are spread out over larger vertical regions. The area under each curve represents the portion of that component which is released into the gas phase during in-flight combustion. Mass that strikes the boundaries is not represented in this graph.

Droplets that strike the wall may be fully combusted (containing only smelt) or partially combusted containing some fractions of water, volatiles, and char. This data can also be summed and presented as a function of vertical position of the furnace. The base case data for wall activity is shown in Figure 8. In the base case, it is observed that most of the droplet mass that does strike a wall lands between 0 and 5 m (below the black liquor guns). The droplets striking the lower walls contain significant portions of char, volatiles, and some water. This mass may account for 20 to 50% of the inorganic black liquor mass depending on mass median diameter and can contain a significant amount of uncombusted char and/or volatiles that would burn on the wall or fall to the bed.

Additional mass impacts the walls from 6 m on up to the top of the combustion zone at 30 m at a gradually decreasing rate. Black liquor droplet mass reaching the walls above the black liquor nozzles did not contain significant portions of uncombusted char or volatiles. Combustion reactions at the walls or mass falling from the walls to the bed are not described in these simulations.

Another way to examine the data which also include bed information is to plot cumulative component mass as a function of vertical height in the furnace. Samples of these graphs are included in Figure 9. The lower curve in each figure represents component mass that strikes the bed ($z=0$) or the walls as a function of vertical position. The upper curve represents total mass including in-flight and wall mass and will approach 1.0 for each component. The offset from 1.0 represents carry-over which is usually less than .02 (i.e., 2%) for smelt and zero for water and combustibles.

Finally, a short table of values for carry-over and component mass to the char bed is computed in each simulation (see Table 5).

Table 5. Summary of Droplet Fates for the Base Case Simulation.

Droplet Fate	Water	Volatiles	Char	Inorganics
In-flight	0.96281	0.80371	0.67394	0
Hit Walls	0.0316	0.1439	0.21063	0.67207
Carried Out	0	0	0.0001	0.01022
Hit Bull Nose	0	0	0	0
Hit Char Bed	0.00557	0.05238	0.11535	0.31751
Totals	1	1	1	1

Mass Mean Diameter Studies

In Figure 10, the carry-over is plotted as a function of the mass median diameter. A similar trend was observed by Grace et al. in earlier simulation studies (5). Two different phenomena occur during black liquor combustion which resulted in most of the observed carry-over. Very small droplets with diameters of about 0.5 mm burn very quickly (complete combustion in <0.5 sec.), and the small smelt bead that is left over is easily entrained in gas flow. These tiny droplets will often be captured in recirculation zones and ultimately strike either a wall or be carried out of the furnace combustion zone (see trajectories in Figure 11).

The second mode of black liquor combustion that can result in significant carry-over occurs when medium-sized droplets are injected at a certain speed and angle so that they enter the high velocity channel just as they go through the final stages of pyrolysis at maximum swollen diameter (see Figure 12). For the flow field used in this study, this type of carry-over phenomenon occurred for droplet diameters of about 3.25 mm injected at 10 m/s at a slight downward angle toward the center of the furnace. Larger droplets are dense enough and have enough momentum to pass through the high velocity channel, while smaller droplets are deflected before they reach the high velocity regions.

A third droplet trajectory that produced carry-over was also observed. Some small droplets moving toward the char bed surface were entrained by fast moving gases from the primary and secondary air ports and were swept upward and out of the furnace in some cases. The initial size of these black liquor droplets was approximately 1 mm. Most droplets swept up in this fashion impacted a wall before they could be carried out of the furnace, however.

The various phenomena that can cause carry-over of black liquor particles can result in a complex relationship when typical droplet diameter distributions are simulated. Highest carry-over rates were observed for the smallest mass mean diameters and lowest carryover rates for the largest diameter droplets. However, the relationship is not a simple monotonic decreasing trend of carry-over with respect to mass mean diameter. There is a local minimum carry-over at about 2.5 mm for the current simulations.

When inorganic mass accumulation on the walls is plotted versus vertical height for each mass mean diameter in the 3-D plot in Figure 13, it is observed that droplets strike the walls of the furnace in all areas, but they are concentrated in two zones. Larger droplets strike the walls lower in the furnace in a zone between 1 and 3 m. Smaller droplets are concentrated between 5 and 8 m, just below the tertiary air level. The explanation for this is that large droplets at moderately high nozzle velocities have trajectories with only small deflections, thus striking adjacent or opposing furnace walls below the liquor nozzle near the secondary jets. The smaller droplets are thrown back against the wall due to recirculating flows caused by the tertiary jets. Evidence in support of this conclusion is the fact that mass on the lower walls contains uncombusted material, while mass striking the walls above the nozzle was primarily inorganic ash only.

As mass mean diameter was increased from 1 to 4 mm, the amount of smelt that lands directly on the bed gradually increased from about 30% to 40%. Uncombusted char that lands directly on the bed increased linearly from 0% at 1.5 mm to 30% at 4 mm. Char to the bed was not significant for diameters of 1.5 mm and less.

Horizontal Spray Angle, Φ

The width of spray pattern was varied from the base case condition of -70° to +70° (spanning 140°) to a narrow spray of -15° to +<15° (spanning 30° total). Simulations were run for mass mean diameters of 1.5 mm, 2.5 mm, and 3.5 mm, with typical size distributions. For the ≈2.5 mm Dm simulations, a narrower spray resulted in a slight increase in carry-over from about 1% to 2.5% of total inorganic (see Figure 14). This seems reasonable since a narrower spray pattern would result in a greater percentage of droplets injected straight at the high velocity gases in the channel. A similar effect was observed for the Dm = 3.5 mm case. However, just the opposite was observed for the smaller Dm = 1.5 mm simulation. A decrease in carry-over from 3% to 0.25% resulted with narrowing of the spray pattern.

It can be concluded that directing the black liquor spray into the center of the furnace results in less mass to the lower walls. In the case of Dm = 1.5 mm, a narrower spray directed into the center caused completely combusted particles to be deflected back to the walls between 5 and 10 m.

Very Narrow Droplet Size Distributions

Very narrow distributions about the mass median droplet diameters between 0.5 mm and 4.0 mm were also examined at conditions of the base case ($\Phi = 70°$, $\theta = -10°$). The narrow size distribution was simulated by using standard deviations one quarter the size of normal spray distributions. Two mm droplets resulted in the least carry-over (see Figure 15). This result is consistent with typical distribution data. However, the 2 mm droplets burned almost completely in-flight sending about 1% unburned char directly to the bed and 8% to the lower walls. When large sizes are used, less combustion occurs in-flight, and the droplets strike opposing walls still wet.

Figure 16 shows the percent carbon by weight in the resulting carry-over as a function of initial droplet diameter for the narrow size distribution simulations. It is clear that carry-over for small diameter droplets (Dm < 2.5 mm) was completely combusted ash and that larger droplets, if conditions caused entrainment, could contain small portions of unburned char. This result helps to differentiate between carry-over of large vs. small droplets.

Vertical Spray Angle, θ

The in-flight results for simulations with varying vertical angles are presented in Figure 17. These figures show the intuitive results that in-flight combustion zones for evaporation, pyrolysis, and char burning move upward with higher angles. The wall behavior is presented in Figure 18. At -30°, the larger droplets strike the bed rather than the walls. At +30°, a very large portion of the droplet mass (70%) strikes walls between 2 and 8 m.

CONCLUSIONS

A fixed-field approach was used to investigate in-flight combustion of black liquor sprays in a recovery furnace geometry. This work supports the findings of previous investigations that found that carry-over is not a monotonic function of black liquor droplet size.

Two different conditions were found to result in higher levels of carry-over for the present simulations. One condition involves entrainment of ash from very small black liquor droplets of 0.5 mm to 1.0 mm caught in recirculating flow patterns. Another condition that resulted in carry-over occurred when black liquor droplets with moderate original diameters (about 3 mm) were entrained in fast moving gases in the furnace as the droplets swelled during pyrolysis. This mode of carry-over resulted in uncombusted carbon being carried out with the inorganic portion of the black liquor.

Changing width of black liquor spray patterns affected combustion behavior by concentrating or diffusing the zone for combustion. Opposite effects on carry-over were observed for small versus large droplet diameters as width of spray pattern was decreased. Large droplets tended to be carried out at greater proportions, small droplets to a lesser degree as a narrower spray pattern was used.

Spraying liquor at higher angles of injection moved combustion activity up in the furnace with less uncombusted volatiles and char going directly to the bed. Spraying at sharp downward angles caused more wet liquor to hit the bed.

REFERENCES

1. Williams, T.J., and Galtung, F.L., "A Mathematical Model of a Recovery Furnace," Proceedings ISA/75, Milwaukee, WI, 1975.

2. Merriam, R.L., Kraft, *ver. 2.0* - Computer Model of a Kraft Recovery Furnace, A.D. Little, Inc., Cambridge, MA, 1980.

3. Shiang, N.T., and Edwards, L.L., "Kraft Recovery Furnace Capacity and Efficiency Improvement," Tappi Int.Rec.Conf., 1985.

4. Shick, P.E., "Predictive Simulation of Recovery Furnace Processes on a Microcomputer," Kraft Recovery Operations Seminar, Orlando, FL., 1986.

5. Grace, T., Walsh, A., Jones, A., Sumnicht, D., and Farrington, T., "Three-Dimensional Mathematical Model of the Kraft Recovery Furnace," CPPA/TAPPI Int. Chem. Rec. Conf., Ottawa, April 1989.

6. Horton, R.R., "In-flight Black Liquor Combustion Modeling - A Parameter Sensitivity Study," Timberline Colloquium on Recovery Boiler Modeling, April 1991.

7. Karvinen, R., Hyoty, P., and Siiskonen, P., Tappi J. 74(12):171-177 (1991).

8. Blackwell, B., Oliver, R., and Briscoe, B., "Physical Flow Modelling of a Vintage Combustion Engineering Kraft Recovery Boiler," CPPA Tech.Sect.Conf., May 1989.

9. Perchanok, M.S., Bruce, D.M., and Gartshore, I.S., "Velocity Measurements in an Isothermal Scale Model of a Hog Fuel Boiler Furnace," JPPS, 15(6):212-219, Nov., 1989.

10. Blackwell, B., "Validity of Physical Flow Modelling of Kraft Recovery Boilers," Timberline Colloquium on Recovery Boiler Modeling, April 1991.

11. Jones, A.K., Chapman, P.J., and Mahaney, J., "Improved Air Port Arrangements for Secondary Air Level," 1991 CPPA Annual Meeting.

12. Siiskonen, P., "Cold Flow Measurements in a Recovery Boiler," Timberline Colloquium on Recovery Boiler Modeling, April 1991.

REFERENCES (continued)

13. Chapman, P., and Jones, A., Tappi Engineering Conference Proc., 1990.

14. Spielbauer, T.M., and Aidun, C.K., Tappi J. 75(2):136, 1992.

15. Adams, T.N., Empie, H.L., Obuskovic, N., and Spielbauer, T.M., Kraft Black Liquor Delivery Systems, DOE Contract No. FC02-88CE40839, Report No. 1, February 1990.

16. Stockel, I.H., Research on Droplet Formation for Application to Kraft Black Liquors, Technical Report No. 1, DOE/CE/40626-T2, March 1985.

17. Walsh, A.R., and Grace, T.M., JPPS. 15(3):84-89(May 1989).

18. Empie, H.L., Lien, S., Yang, W., and Adams, T.N., Kraft Black Liquor Delivery Systems, DOE Report #3, DE-FC02-88CE40839, in press.

19. Frederick, W.J., Combustion Processes in Black Liquor Recovery, Report No. 1, DOE Contract No. AC02-83CE40637, March 1990.

20. Empie, H., Grace, T., Frederick, W., Horton, R., Nichols, K., Medvecz, P., and Verrill, C., Black Liquor Combustion, Report No. 1, DOE Contract No. DE-FG02-90CE40936, in press.

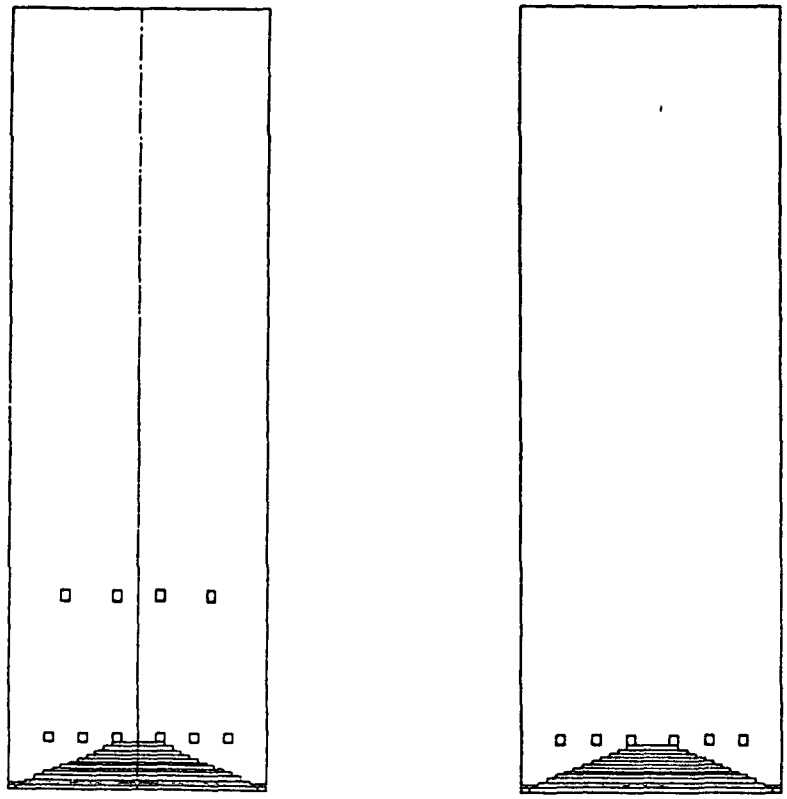

Figure 1. Front and Side Elevation Schematic of Furnace Geometry for CFD Calculations.

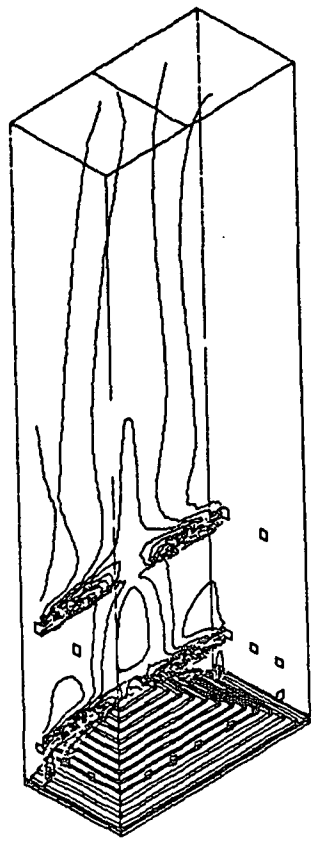

Figure 2. Velocity Magnitude Contours in a Vertical Plane Through Secondary and Tertiary Ports.

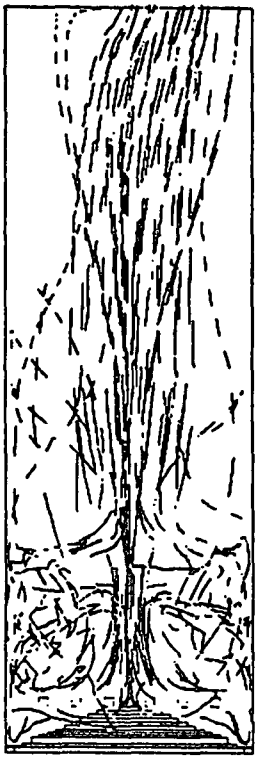

Figure 3. Trajectories of Air Parcels Released at the Secondary Air Ports.

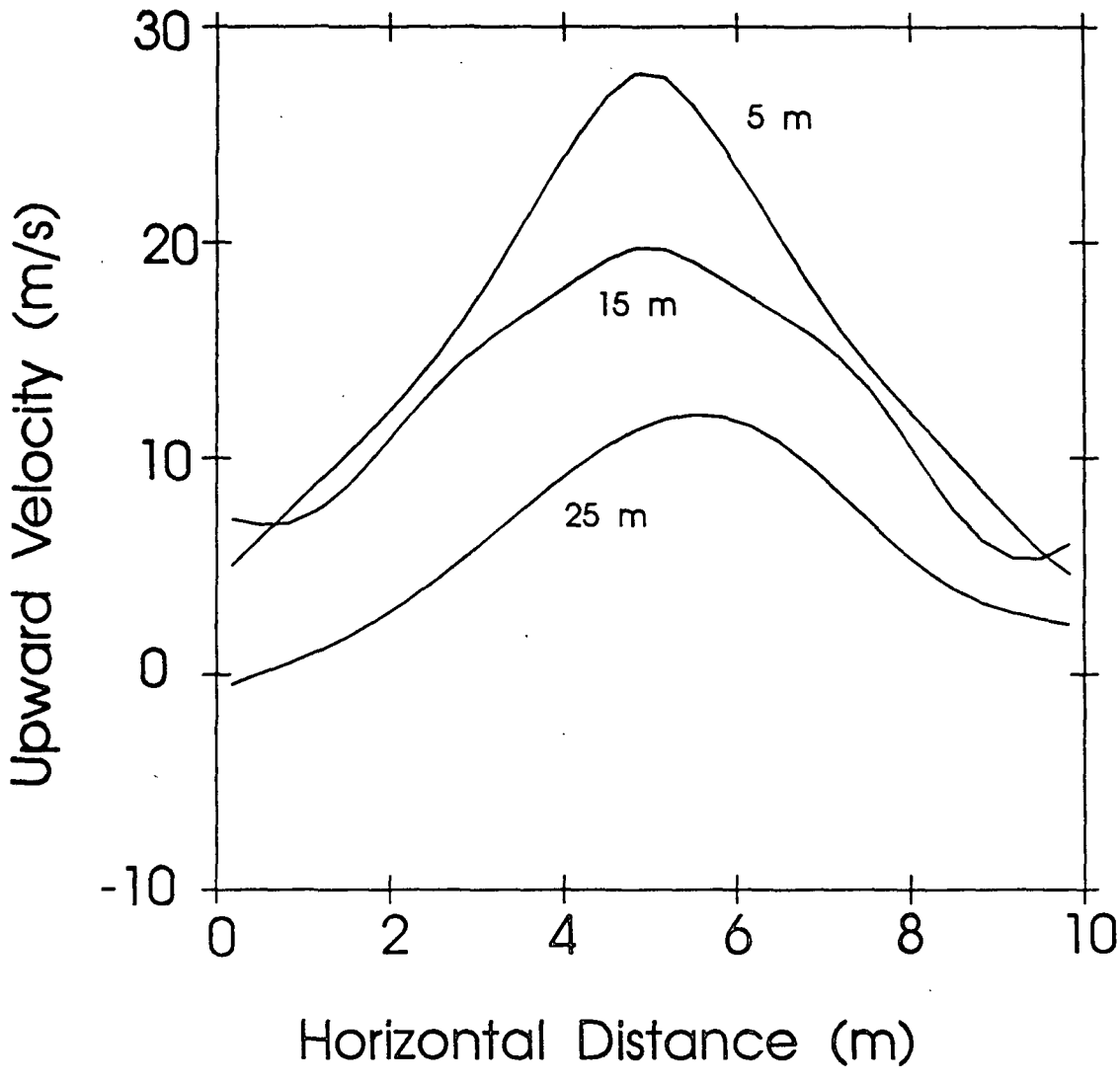

Figure 4. Vertical Velocity Components at Three Levels in the Furnace.

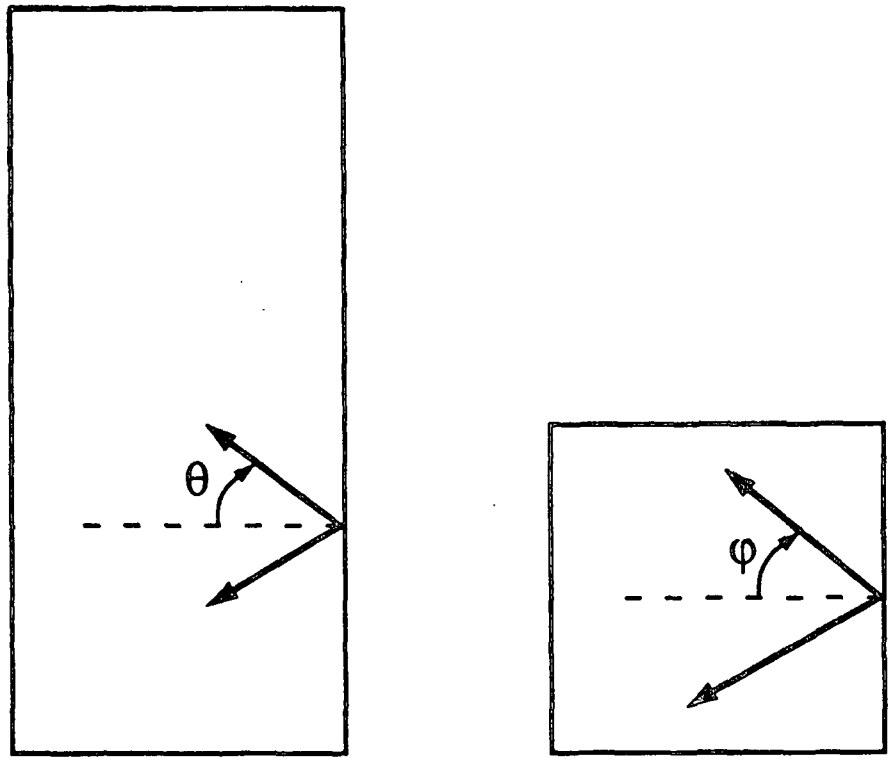

Figure 5. Top and Side Views of Black Liquor Nozzle Spray Angles.

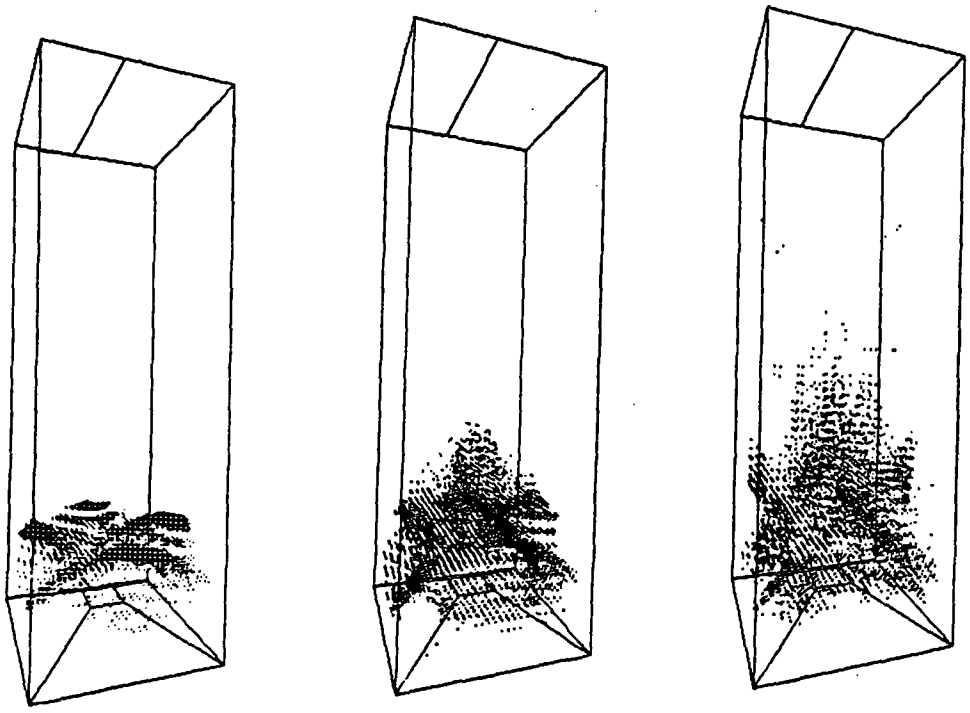

a) Evaporation Rate b) Pyrolysis Rate c) Char Burning Rate

Figure 6. Three Dimensional Views of Evaporation, Pyrolysis, and Char Burning Activity for the Base Case.

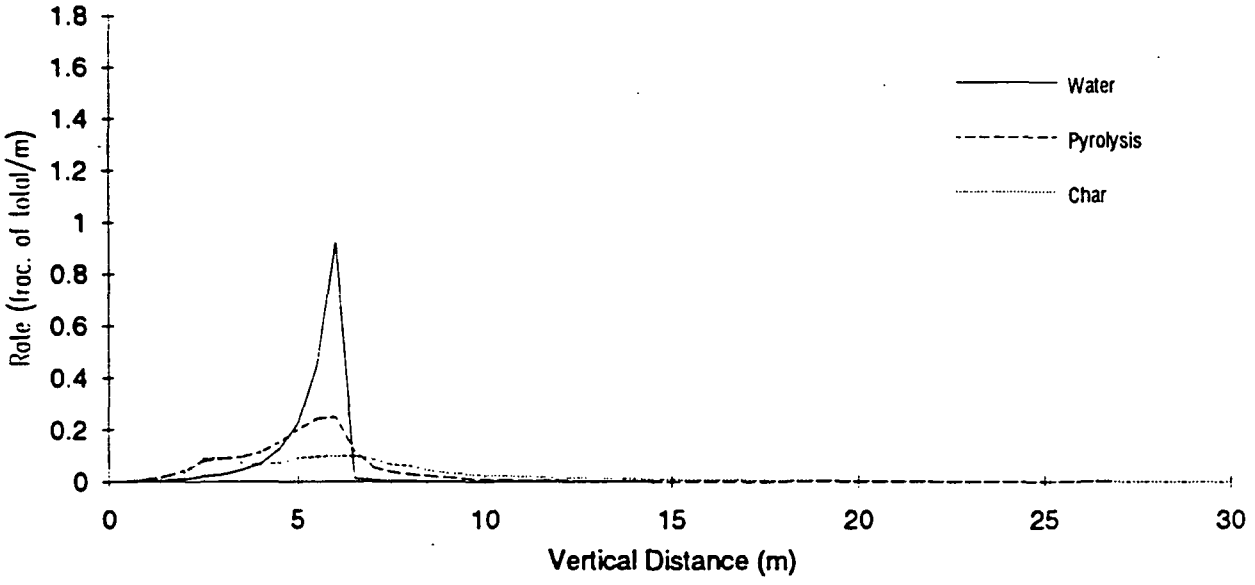

Figure 7. In-flight Combustion Rates as a Function of Vertical Position in the Furnace for the Base Case.

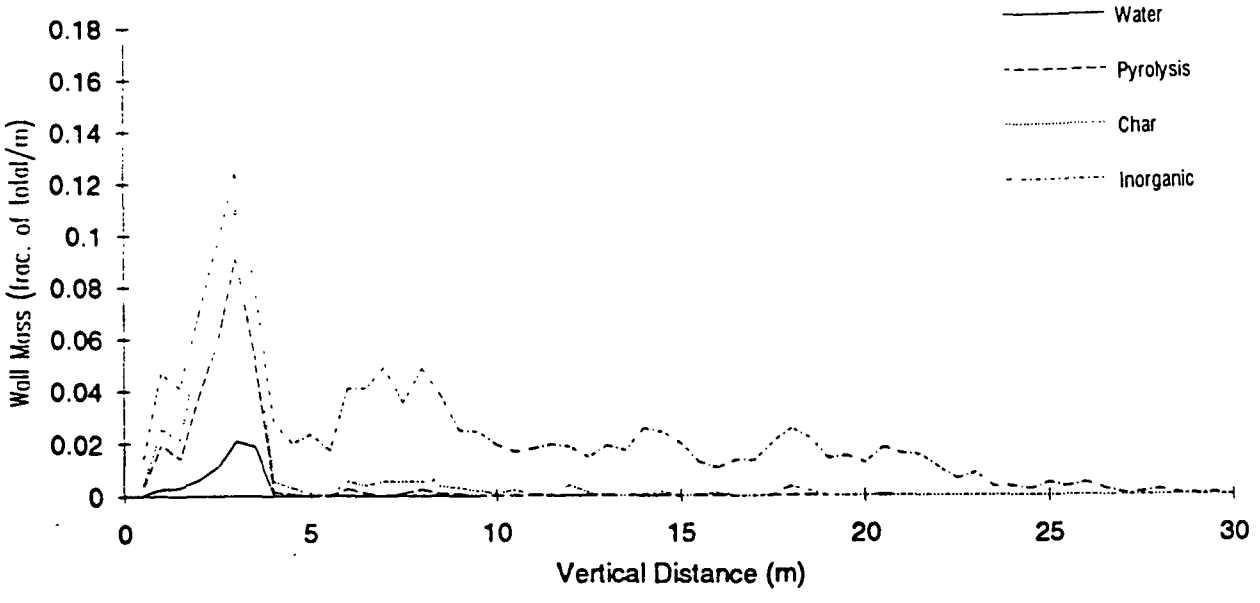

Figure 8. Black Liquor Mass that Strikes the Walls as a Function of Vertical Position in the Furnace.

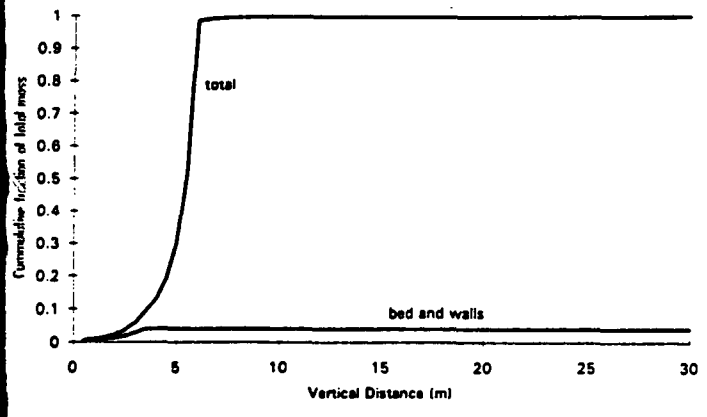

a) Evaporation

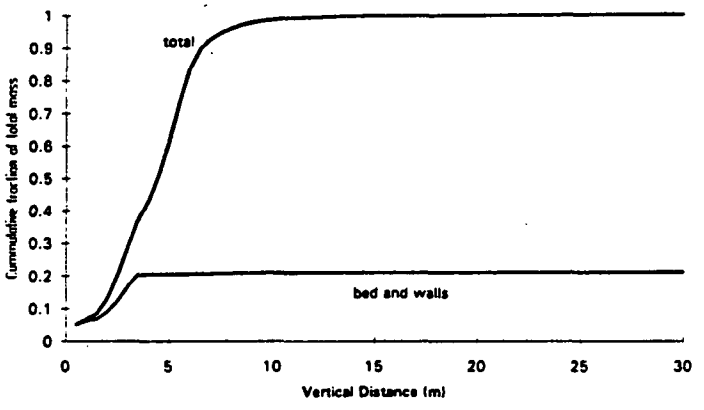

b) Pyrolysis

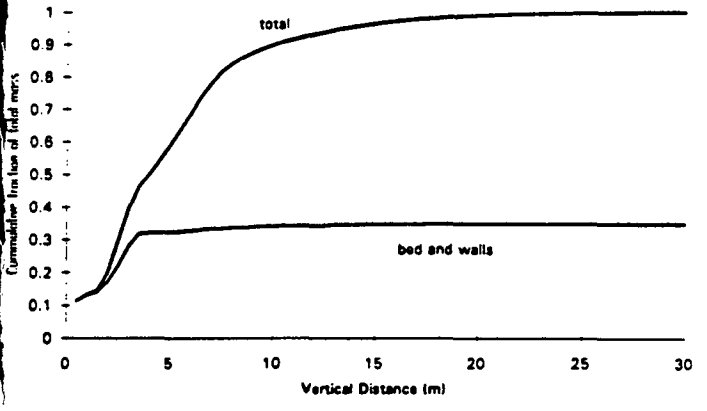

c) Char Burning

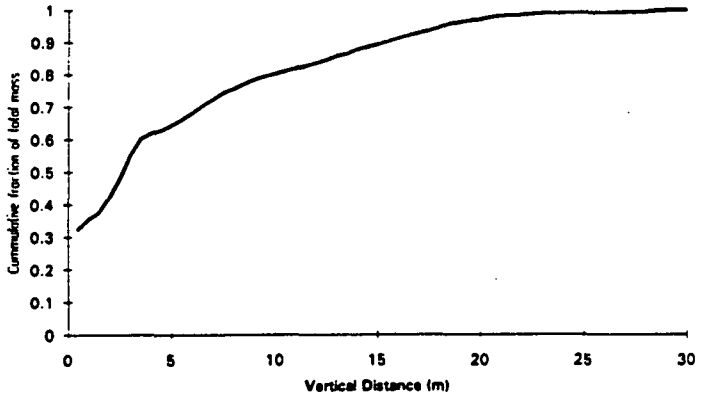

d) Inorganic Ash

Figure 9. Cumulative Mass Plots for the Four Stages of Black Liquor Combustion as a function of Vertical Position in the Furnace.

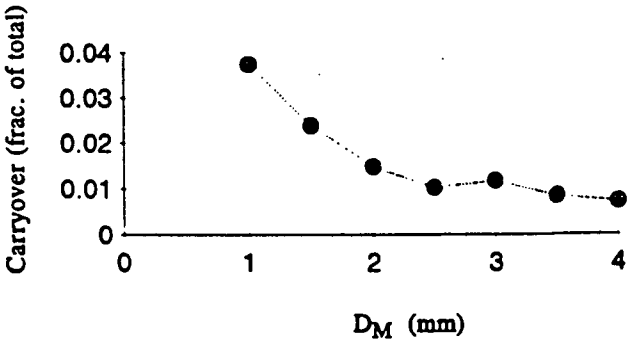

Figure 10. Carryover versus Mass Mean Diameter.

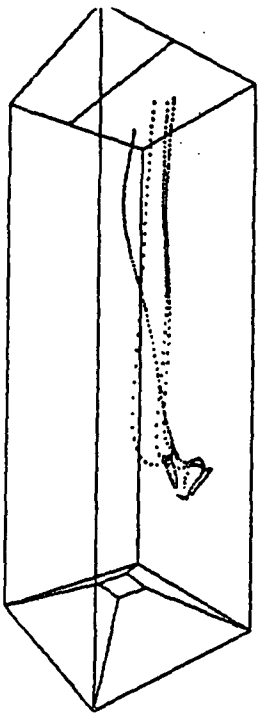

Figure 11. An Example of Small Droplet Trajectories that Result in Carryover.

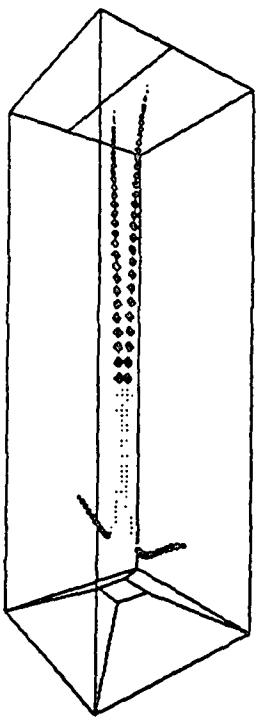

Figure 12. An Example of Large Droplet Trajectories that Result in Carryover.

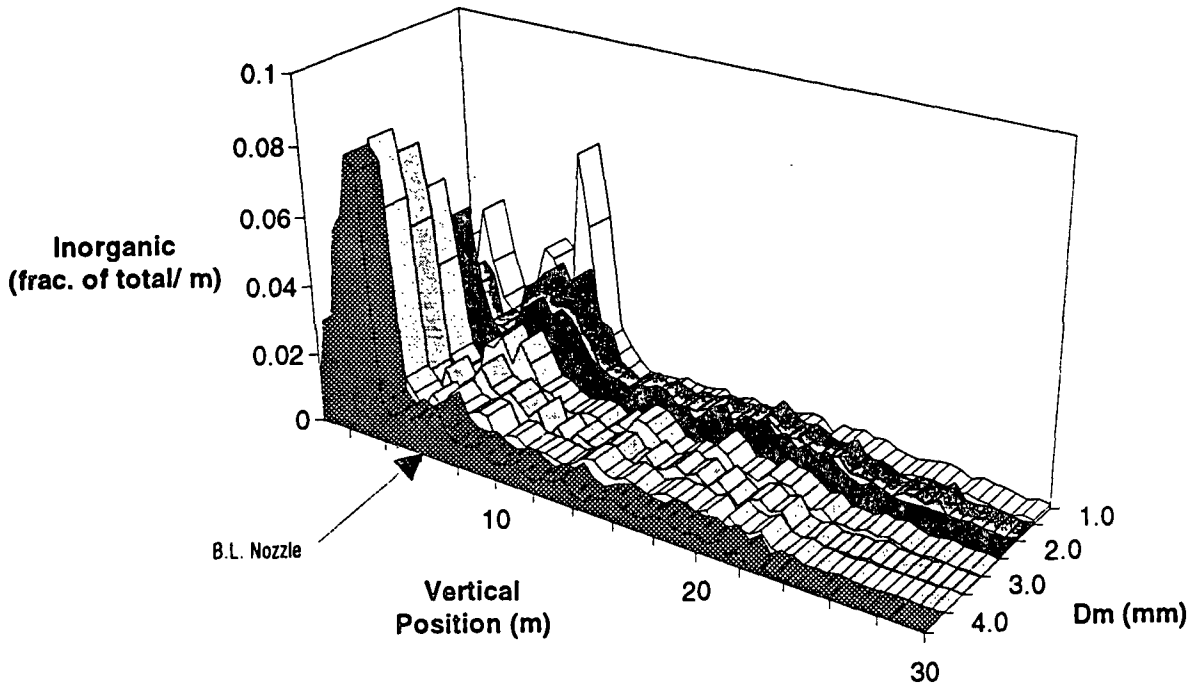

Figure 13. Inorganic Ash that Strikes the Walls as a Function of Droplet Size and Vertical Position in the Furnace.

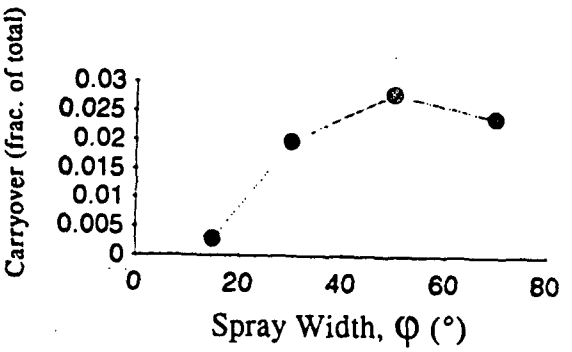

a) Dm = 1.5mm

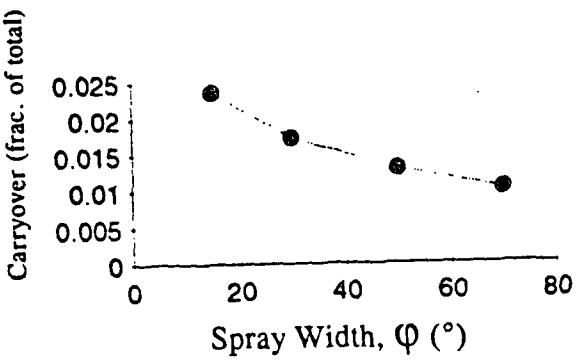

b) Dm = 2.5mm

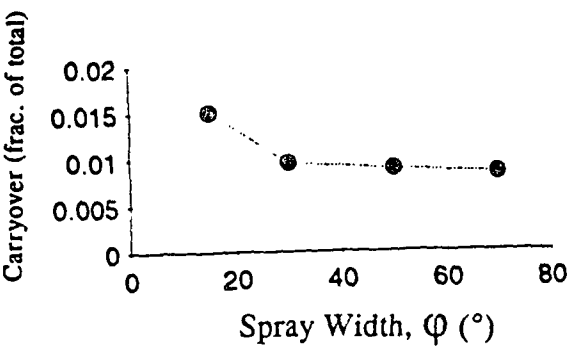

c) Dm = 3.5mm

Figure 14. Carryover versus Width of Spray Pattern for Three Mass Mean Diameters.

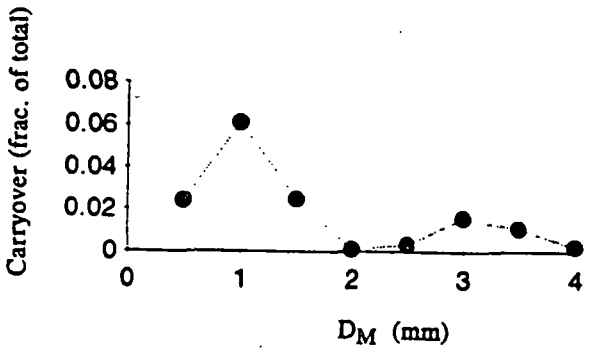

Figure 15. Carryover versus Diameter for Very Narrow Distributions.

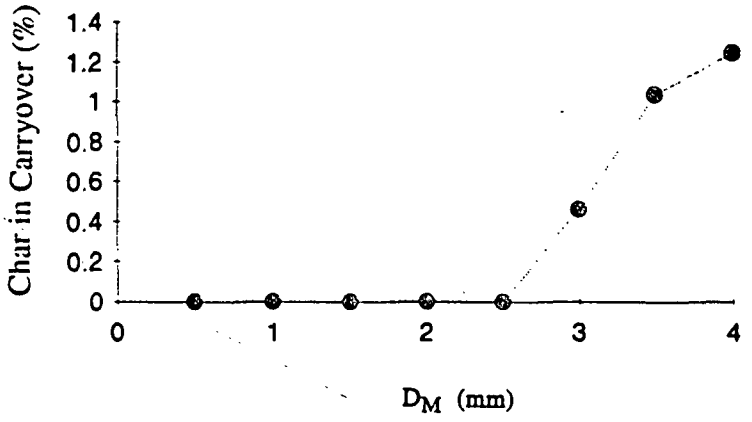

Figure 16. Amount of Char in Carryover as a Function of Droplet Size.

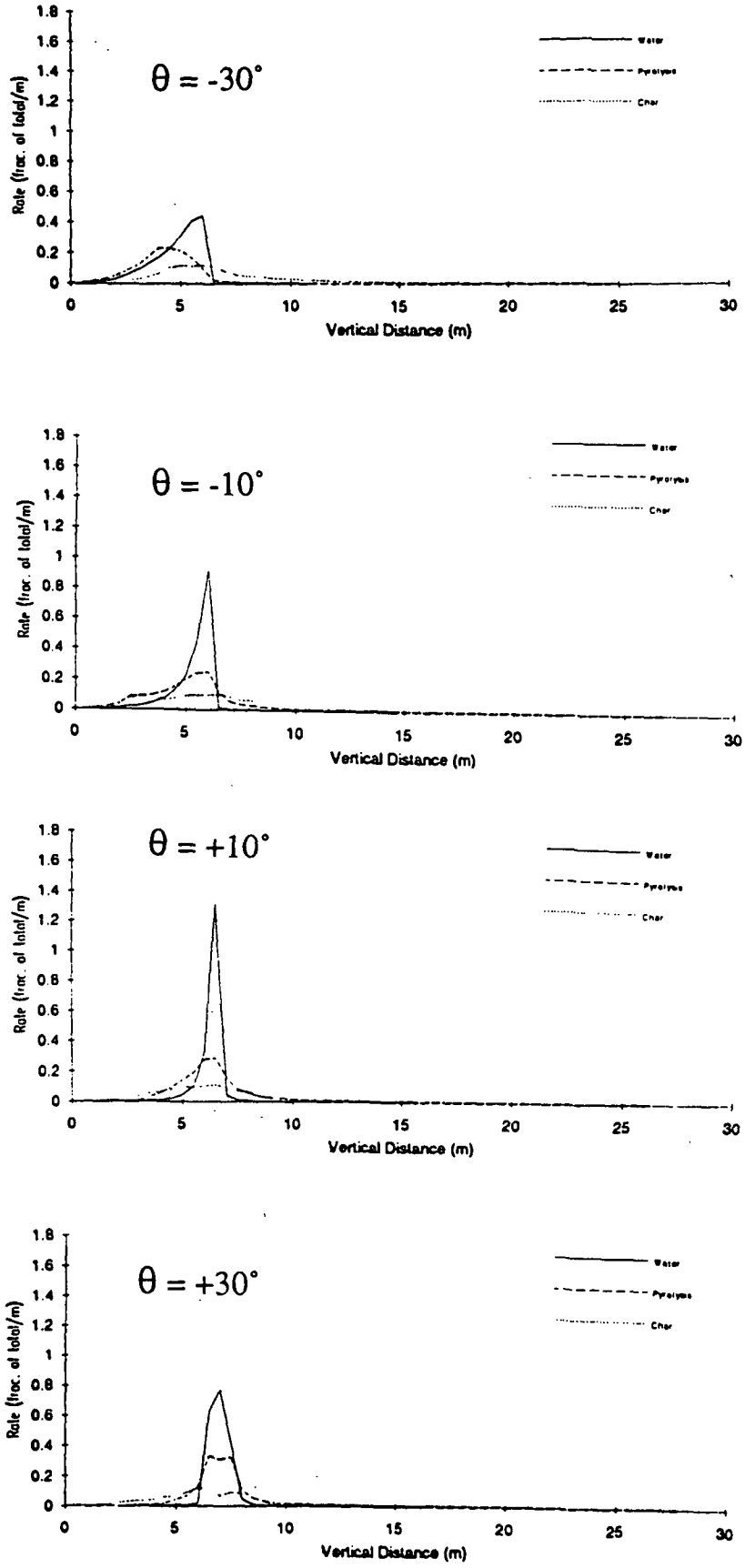

Figure 17. In-flight Combustion Rates for Several Vertical Firing Angles.

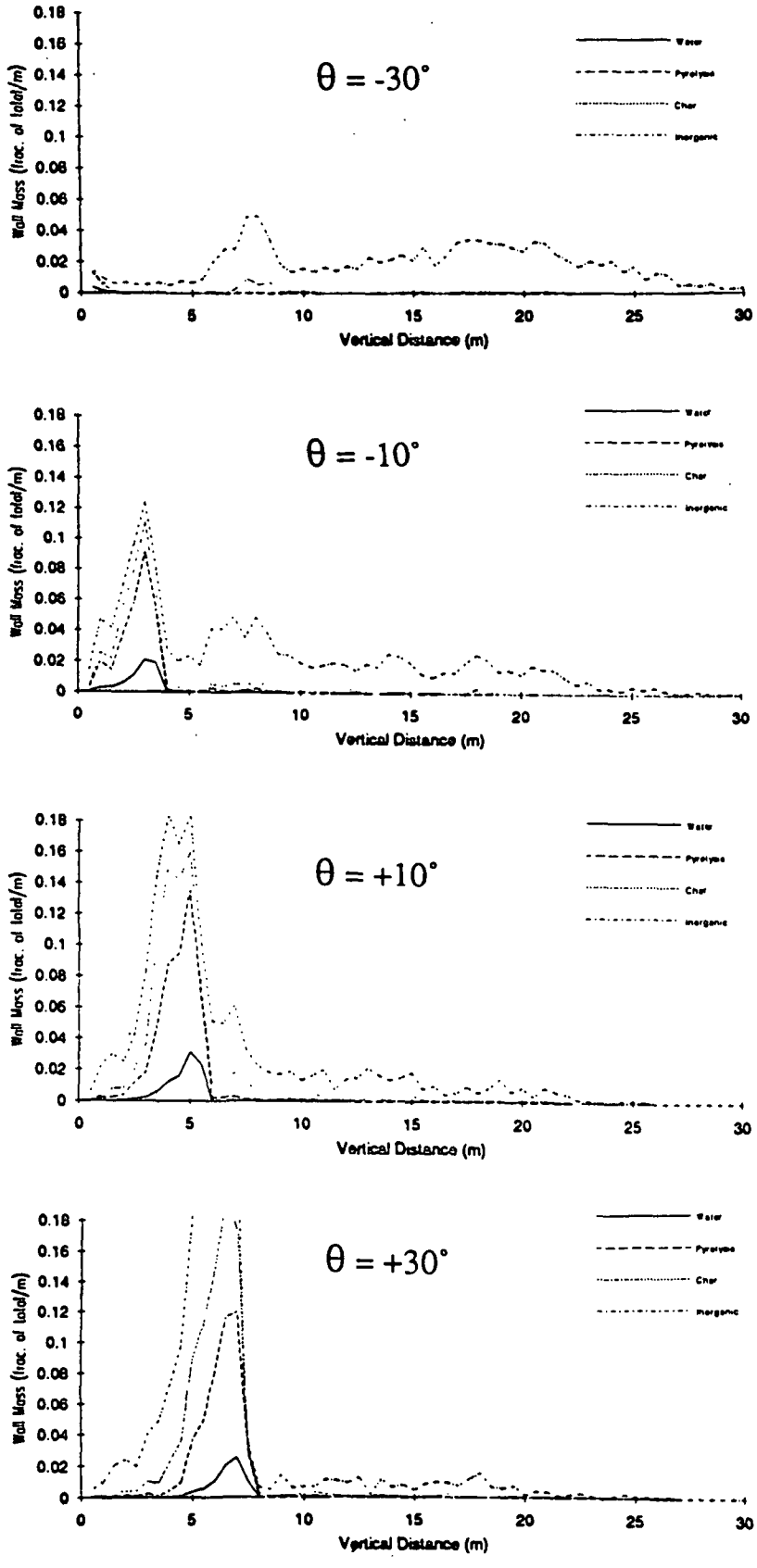

Figure 18. Black Liquor Mass that Strikes the Walls as a Function of Vertical Firing Angle.